ACS OMEGA

http://pubs.acs.org/journal/acsodf

Article

Experimental Investigation of the Flow Characteristics in Crude Oil Containing Sand and Gas Flowing Along Vertical Pipelines

Dong Zhang, Shuo Liu,* Jian Zhang, Lin-tong Hou, and Jing-yu Xu*

Cite This: https://dx.doi.org/10.1021/acsomega.0c04637

Read Online

ACCESS | Metrics & More | Article Recommendations

ABSTRACT: An experimental study on the flow behavior of crude oil containing sand and air in a vertical pipe with 50 mm diameter was carried out. The experiments were conducted under the following input superficial phase velocities: oil from 0.1 to 2.23 m/s and gas from 0 to 0.34 m/s. Oil was blended with sand in three different volume concentrations, namely, 0.7, 2, and 3%. Two different types of sand were used to investigate the effect of sand size distribution. A comparison between rheological measurements and pipe flow data showed that the stress−strain relationship obtained by the rheometer could be used to predict the transport characteristics in the vertical pipe flow. It was demonstrated that a small gas injection and sand addition can decrease the total pressure and friction pressure gradients. In the oil flow, the injection of air generally increased the friction factor compared to the single-phase flow, especially at low Reynolds numbers. However, the friction factor decreased by adding a small amount of fine sand. The accuracy of the correlation developed in this study was compared with other three correlations widely used in gas−liquid vertical pipe flow.

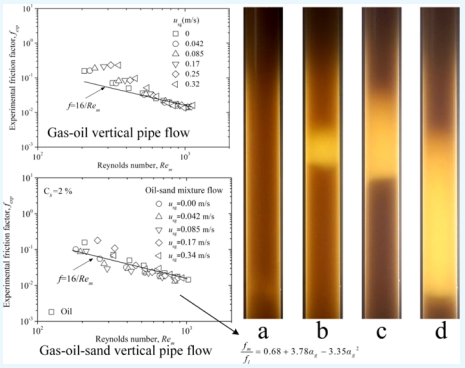

INTRODUCTION

In the process of petroleum exploitation and transportation, oil−gas−sand vertical flow often occurs. As the output crude oil produced from well heads usually entrains sand, clay, or other porous solids, crude oil with sediment grain exhibits more complex flow characteristics compared to crude oil without sediment grain. In an extreme case, the output crude oil entraining sand may be up to 5% of the total volume.[1,2] However, the sand volume concentration of the output crude oil[3] can be as low as 0.014−0.11 kg/m^3. Usually, the sand entrained by crude oil could have an adverse effect on productivity as its transport exacerbates pipeline erosion. If the hoist velocity is not sufficiently high, the solid particles will be settling at the bottom of the vertical tube and thus constrict the flow of crude oil. Although sand removal techniques have been successfully used for fluidizing the settled sand particles and removing them from the wellbore, the related downhole sand exclusion systems are expensive to operate.[4]

In fact, the total pressure gradient can be influenced by adding a small amount of fine sand as viscosity changes with the addition of sand.[5−7] Several studies have been conducted on gas−liquid−sand three-phase vertical flow characteristics.[2,8−11] Erian and Pease[11] proposed a slightly different approach for predicting the pressure gradient for the gas−liquid−solid three-phase flow through a vertical pipe. The three-phase pressure gradient correlation consists of two parts: a combination of a modified one-dimensional, two-fluid annular dispersed flow model and a one-dimensional pneumatic conveying model. Adeyanju and Oyekunle[2] presented an oil−gas−sand flow pressure gradient model comprising the fluid flow pressure gradient and the pressure gradient due to transportation of sand in the fluid flow. Although some studies have focused on three-phase flow characteristics in vertical pipes, the influence of gas injection and sand addition on the pressure drop of the vertical pipe flow has not been adequately investigated. In fact, the injection of gas in the hydraulic transport of sand in a vertical pipe flow may increase or decrease the pressure gradient.[9,12] Moreover, previous model performs well in slurry conditions which did not exhibit non-Newtonian properties.[13] When encountered with non-Newtonian mixtures, the availability of models needs careful concentration.

On the basis of discussions above, the aim of this study is to comprehensively understand the effect of gas injection and sand addition on the flow characteristics of vertical oil flow in consideration of non-Newtonian properties. The paper is organized as follows. In the first section, the rheological properties of oil−sand mixtures for different samples and the volume concentrations are measured using a rheometer. In the second section, the influence of gas injection and sand addition

Received: September 21, 2020
Accepted: November 17, 2020

on the flow characteristics of vertical pipe flow is investigated. In the last section, a new model based on Herringe and Davis's correlation is suggested following a brief review of the previous related work.

RESULTS AND DISCUSSION

Oil Containing Sand Flow. In liquid−solid transportation, precise measurement of the apparent viscosity is highly important for estimating the flow pressure gradient. The viscosity curves of hydraulic oil containing sand for different volume concentrations and different samples are shown in Figures 1 and 2, respectively, where it is demonstrated that

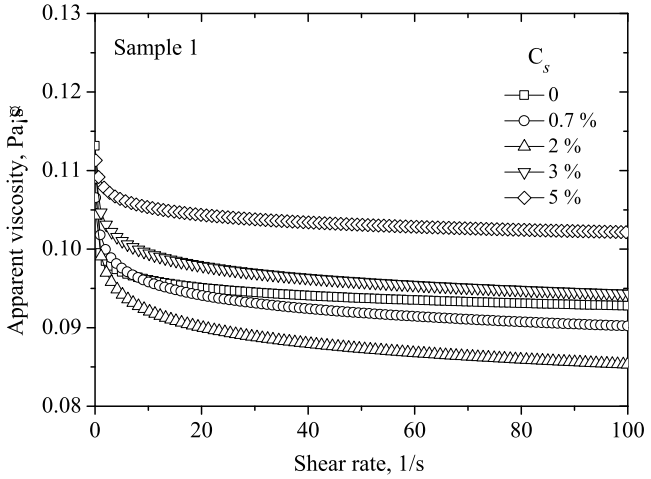

Figure 1. Viscosity curves of sample 1 with different sand volume concentrations at 23 °C.

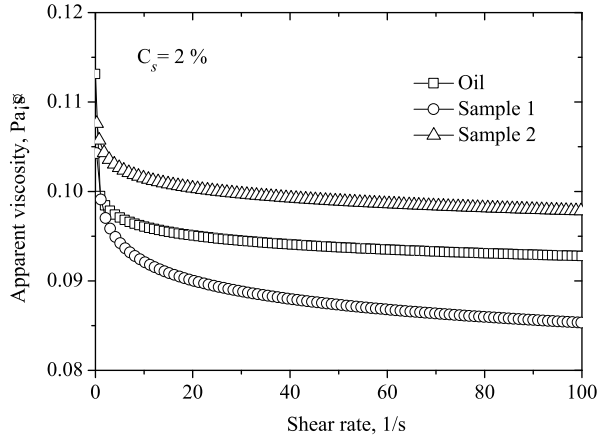

Figure 2. Viscosity curves of hydraulic oil containing sands for two different samples at 23 °C.

after hydraulic oil is blended with sand, all samples exhibit shear-thinning behavior. The apparent viscosity also increases with the particle size at a fixed volume concentration.

When the volume concentration is lower than 3%, the apparent viscosity of oil containing sand is lower than that of pure oil. In fact, when oil is blended with a small amount of fine sand, the apparent viscosity of the mixture decreases. As shown in Table 1, the flow behavior index decreases as the volume concentration increases, before reaching a minimum value. After this point, the flow behavior index increases steadily with a further increase in the volume concentration.

Table 1. Parameters Extrapolated by the Power-Law Model for Oil−Sand Mixtures

sample	C_s (%)	k (Pa·s^n)	n	R^2
oil	0	0.09949	0.9848	0.999
sample 1	0.7	0.1018	0.9737	0.999
	2	0.0995	0.9670	0.998
	3	0.1049	0.9769	0.999
	5	0.1086	0.9867	0.998
sample 2	2	0.1053	0.984	0.999

This can be explained by the fact that at low volume concentrations, the hydraulic oil blended with sand becomes more shear-thinning, and thus the apparent viscosity decreases. However, with a further increase in the sand volume concentration, the interfacial interaction between the particles could be enhanced, which leads to a rise in the apparent viscosity. Thus, these two opposite trends lead to an apparent viscosity that may be lower or higher than that of pure oil.

Compared with oil pipe flows, oil−sand mixture liquids always show different flow characteristics owing to their complex rheological properties. Thus, it is important to clarify the effect of sand on the oil pipe flow. The total pressure gradient and the frictional pressure gradient of sample 1 for different volume concentrations are shown in Figure 3a,b, respectively. It can be seen that when the volume fraction is 0.7 and 2.0%, the total pressure gradient of oil−sand mixture is less

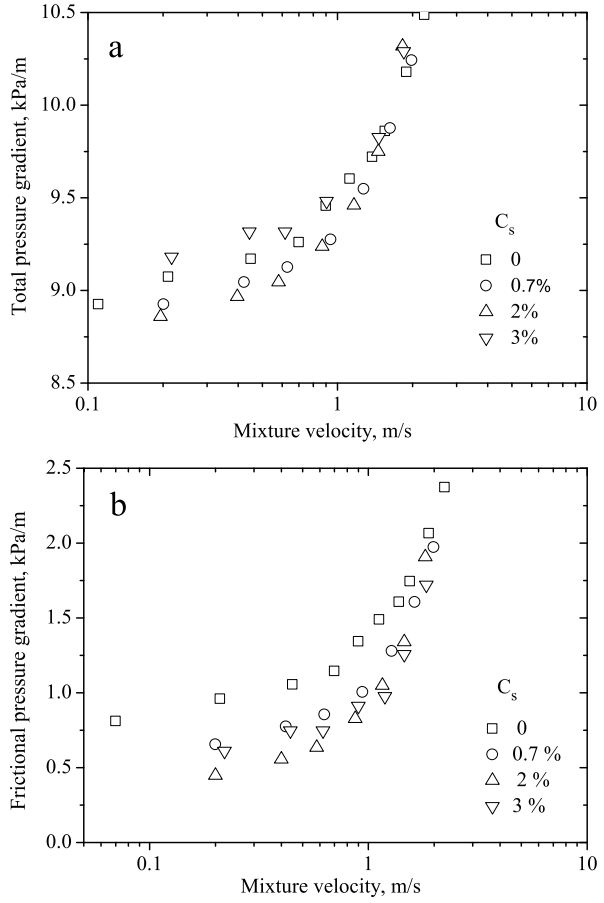

Figure 3. Pressure gradient against the oil−sand mixture velocity at three different volume concentrations for sample 1: (a) total pressure gradient and (b) frictional pressure gradient.

https://dx.doi.org/10.1021/acsomega.0c04637
ACS Omega XXXX, XXX, XXX−XXX

than that of pure oil, and when the volume fraction reaches 3.0%, the total pressure gradient of oil−sand mixture is larger than that of pure oil; when the volume fraction is 0.7, 2.0 ,and 3.0%, the friction pressure gradient is smaller than that of pure oil−sand mixture. This may be attributed to the fact that adding a small amount of sand to the hydraulic oil can reduce the apparent viscosity. However, once the volume fraction of sand is too large, the friction pressure gradient increases inversely. On the one hand, the interfacial interaction between these particles becomes larger and larger. At the same time, the addition of sand will increase the density of mixture, which will lead to the increase of total pressure gradient.

The size and distribution of sand particles also have a significant influence on the flow of liquid−solid mixtures. Figure 4 shows the change in the pressure gradient as the

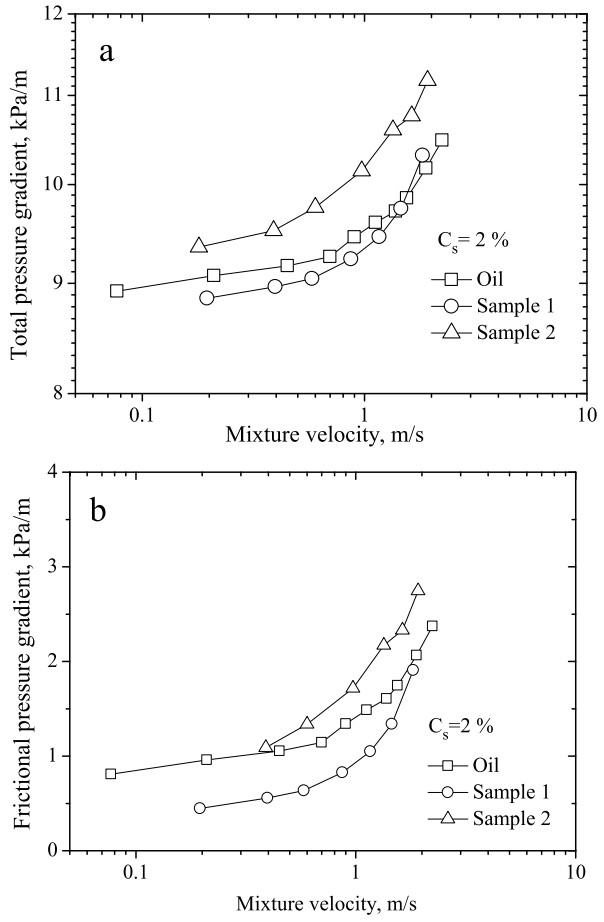

Figure 4. Pressure gradient against the oil−sand mixture velocity at volume concentrations 2% for two different samples: (a) total pressure gradient and (b) frictional pressure gradient.

mixture velocity increases for two different samples. Clearly, larger particle size results in greater pressure gradient. This result is the same as that of a rheometer. This is because fine sand particles are evenly distributed in hydraulic oil, forming a new dispersion system, which leads to the decrease of the viscosity of oil−sand mixture. However, when large particles are added, they will not be evenly distributed in hydraulic oil. Uneven sand particles will enhance the interfacial interaction between the particles, leading to a rise in the apparent viscosity. Therefore, the viscosity of oil−sand mixture with larger sand particles is higher than that of pure oil. At the same time, the drag reduction of fine particles decreases with the increase in the velocity of mixed liquid.

In Figure 5, the friction factor is plotted as a function of the Reynolds number. The experimental friction factor is close to

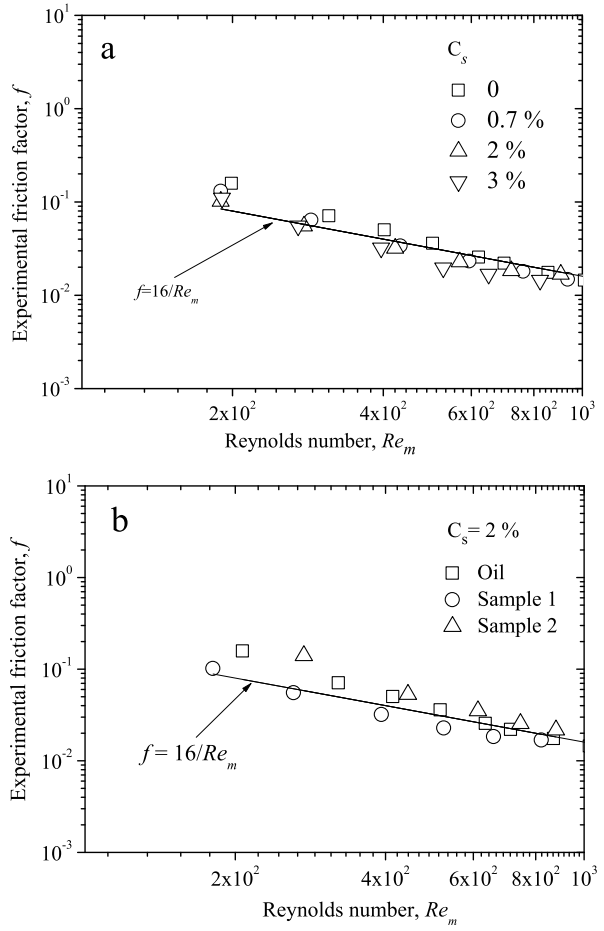

Figure 5. Experimental friction factors as a function of the oil−sand mixture Reynolds number: (a) for different volume concentration and (b) for different samples.

the value by the empirical Poiseuille equation for high mixture Reynolds numbers. The experimental friction factor deviates from the values by the Poiseuille equation for low mixture Reynolds numbers. The results also show that the friction factor initially decreases and then increases with the sand volume concentration and the particle size for a constant Reynolds number. This is because oil becomes more shear-thinning with the addition of fine particles.

For laminar flow of power-law fluids in vertical pipes, the shear stress and shear rate can be calculated by eqs A.13 and A.14. To further study the relationship between the rheological properties and pipe flow, a comparison between the flow curves measured by the rheometer and those obtained during pipe flow at 23 °C for different volume concentrations is shown in Figure 6. It can be seen that the values of shear stress measured by the rheometer are collinear with those obtained by pipe flow. That is, the flow curves measured by the rheometer can be used to predict the shear stress in the pipe flow. Moreover, as the sand volume concentration increases, the shear stress obtained by the pipe flow is larger compared to that obtained by using the rheometer at a low shear rate (for

https://dx.doi.org/10.1021/acsomega.0c04637
ACS Omega XXXX, XXX, XXX−XXX

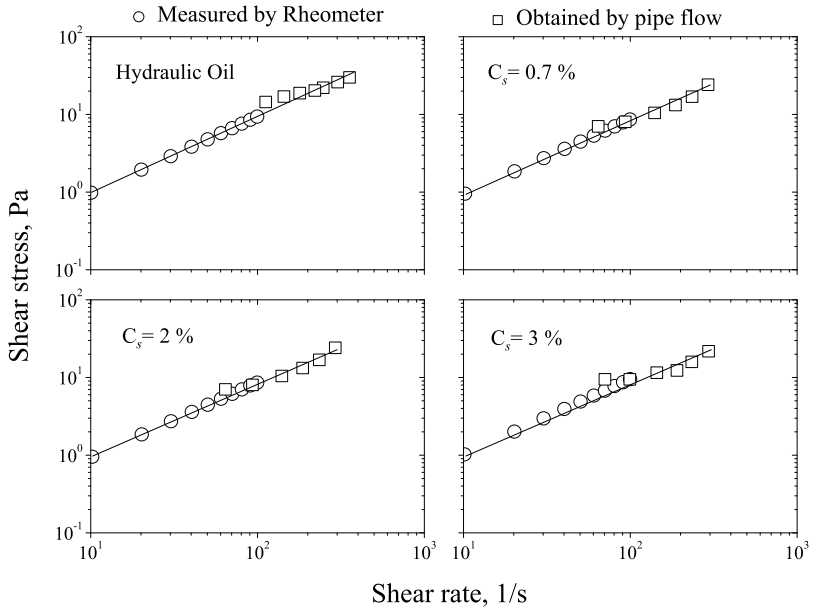

Figure 6. Comparison between the flow curves measured by the rheometer and those obtained by pipe flow.

pipe flow). This is primarily because the sand has settled at a low velocity in the pipe flow.

Oil and Gas Flow. To investigate the influence of gas injection on the flow characteristics of hydraulic oil, flow pattern experiments were conducted in several test runs. Under the studied velocity and gas volume fraction, only bubbly flow (Figure 7a) and intermittent flow (Figure 7b,d) occurred because the mixture velocity of gas and oil was low (u_m < 2 m/s) and the oil phase viscosity was high (95 mPa·s).[12,14]

Gas−liquid flow is common in pipe flows.[15] Gas injection can change the pressure gradient of oil flow in pipes. Figure 8a shows the relationship between the total pressure gradient and the superficial oil velocity at a fixed superficial gas velocity. It can be observed that the total pressure gradient increases with the oil flow rate. Furthermore, the total pressure gradient decreases dramatically as the superficial gas velocity increases for oil velocity below 1.0 m/s. However, when the superficial oil velocity increases, the effect of gas injection on drag reduction diminishes. It can be concluded that drag reduction occurs only at a low superficial oil velocity. Figure 8b shows the effects of the superficial oil velocity on the frictional pressure gradient at different superficial gas velocities. It can be observed that the frictional pressure gradient initially decreases with superficial oil velocity and attains a minimum value. Once this critical velocity is exceeded, the frictional pressure gradient increases gradually. This may be because the viscosity of two-phase oil−gas mixture decreases as the superficial gas velocity increases, thus leading to a decrease in the pressure drop. However, increasing the gas flow rate could also enhance the disturbance imposed on the liquid phase, thus leading to an increase in the two-phase pressure drop. Therefore, when gas is injected into a vertical pipe flow of oil at a fixed superficial oil velocity, these two opposite trends result in a pressure gradient that may be lower or higher than that of pure crude oil.

The experimental friction factor versus the Reynolds number for oil−gas two-phase flow is shown in Figure 9. Here, the experimental friction factor is calculated using the measured frictional pressure drop. As the superficial gas velocity increases, the friction factor maintains a continuous increase.

Figure 7. Experimental oil−air two-phase flow behavior observed through a transparent Perspex tube when the superficial gas velocity is 0.17 m/s: (a) bubble flow, u_{sl} = 2.16 m/s, (b) bubble flow, u_{sl} = 1.50 m/s, (c) intermittent flow, u_{sl} = 0.68 m/s, and (d) intermittent flow, u_{sl} = 0.20 m/s.

As mentioned earlier, as the gas superficial velocity increases, the disturbance imposed on the liquid phase by the gas is accentuated, and thus the friction factor increases. It should be noted that an acceptable prediction is obtained when the Reynolds number is larger than 500. However, when the Reynolds number is lower than 500, the predictions are poor, and they become poorer with higher superficial velocity.

https://dx.doi.org/10.1021/acsomega.0c04637
ACS Omega XXXX, XXX, XXX−XXX

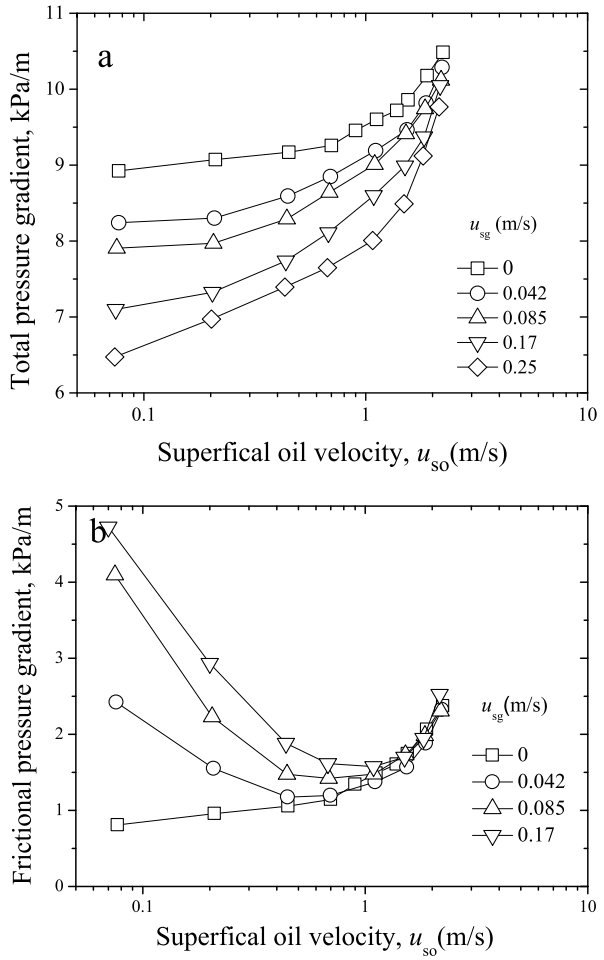

Figure 8. Pressure gradient against the superficial oil velocity at a fixed superficial gas velocity: (a) total pressure gradient and (b) frictional pressure gradient.

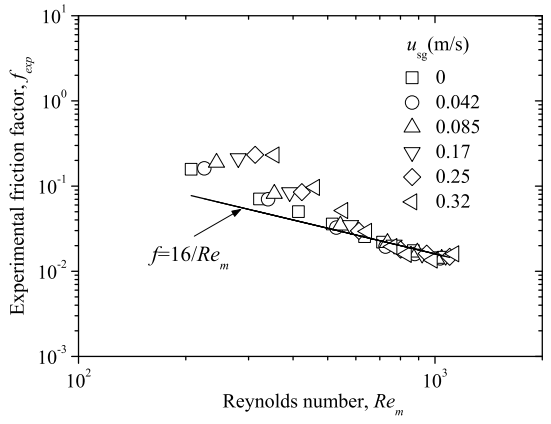

Figure 9. Experimental friction factor versus Reynolds number in the laminar flow.

Oil Containing Sand and Gas Flow. For oil containing sand and gas flow, the most common approach is to treat the oil–sand "double phase" as the "liquid" phase, so that the three-phase flow can be regarded as a gas–liquid mixture, and the analysis can be performed using two-phase correlations.[9,13,16] Gillies et al. investigated the flow characteristics of gas–liquid–solid in horizontal oil wells, and the slurry was treated as a single-phase liquid. Rahman et al. presented an improved implementation of the modified L–M correlation. In their studies, the first modification was to assume that the liquid–sand mixture behaves as a single phase. As the sand particle volume concentration ranged from 0.7 to 3% and the oil phase viscosity was high, the oil–sand mixture was treated as a single-phase liquid that will not cause much error.

For a gas–liquid pipe flow, when the gas phase is of predominance, researchers tend to develop correlation involving the gas friction factor (f_m/f_g) to discuss the flow characters. For instance, in the investigation of effect of drag-reduction polymers in gas–liquid pipe flow, Al-sarkhi and Hanratty,[17,18] Al-sarkhi et al.,[19] and Fernandes et al.[20] applied the above correlation when the gas superficial velocity ranged from 14 to 40 m/s, while the liquid superficial velocity was no larger than 0.2 m/s. When the void fraction is lower, researchers tend to apply correlation involving liquid fraction factor on the basis of experimental data. For instance, Herringe and Davis[21] developed a friction factor correlation involving the liquid friction factor (f_m/f_l) and the void fraction for bubble upward flows. The proposed model is described by eq 1, which is based on pipes whose diameter is 25 mm, where the Reynolds number is defined on the basis of the liquid viscosity. Reasonable agreement between predicted versus experimental data was achieved.

$$\frac{f_m}{f_l} = 1 + 0.22\alpha_g + 0.82\alpha_g^2 \quad (1)$$

where $f_l$is the fraction factor of liquids or sand–liquid mixture.

Based on the assumptions of Marié,[22] Descamps et al.[23] developed a predictive model for mixture friction factor for a vertical flow. This model is presented as follows

$$\frac{f_m}{f_l} = 1 + \frac{10}{3(1-\alpha_g)}\sqrt{1.1\alpha_g}\,\frac{0.25}{u_m}(1-\alpha_g) \quad (2)$$

Moreover, in order to investigate the effect of gas injection on the flow characteristics of immiscible liquids, Xu et al.[12] also developed a fraction factor correlation based on Herringe and Davis's correlation. The assumption is that for the mixture of oil and water as a single liquid phase, the relationship can be expressed as

$$\frac{f_m}{f_l} = \frac{1-\alpha_g}{1 - 3.8\alpha_g + 5.28\alpha_g^2} \quad (3)$$

When the liquid phase is a power-law fluid, Metkin and Sokolov[24] recommended:

$$\frac{f_m}{f_l} = (1-\alpha_g)\left[1 + 2.4n\left(\frac{u_g}{u_l}\right)^{0.5}\mathrm{Re}_l^{-0.0625n}\right] \quad (4)$$

where

$$\mathrm{Re}_l = \frac{8u_l^{2-n}D^n\rho_l}{m\left(\frac{6n+2}{n}\right)^n} \quad (5)$$

Table 2 presents these models for predicting the friction factor of gas–liquid two-phase flow in a vertical tube. In order to compare the predicted friction (f_{pred}) with the experimental data (f_{exp}), we use the following two commonly used statistical parameters (García et al. 2003). The statistical parameters can be expressed as follows

https://dx.doi.org/10.1021/acsomega.0c04637
ACS Omega XXXX, XXX, XXX–XXX

Table 2. Correlations for Predicting the Friction Factor of a Vertical Flow

researcher	correlation
Herringe and Davis (1978)	$f_m/f_l = 1 + 0.22\alpha_g + 0.82\alpha_g^2$
Metkin and Sokolov (1982)	$f_m/f_l = 1 + 2.4n(u_g/u_l)^{0.5}Re_l^{-0.0625}$
Descamps et al. (2008)	$\frac{f_m}{f_l} = 1 + \frac{10}{3(1-\alpha_g)}\sqrt{1.1\alpha_g}\frac{0.25}{u_m}(1-\alpha_g)$
Xu et al. (2012)	$\frac{f_m}{f_l} = \frac{1-\alpha_g}{1-3.8\alpha_g+5.28\alpha_g^2}$

$$E_1 = \frac{1}{n}\sum_{i=1}^{n}|r_i| \tag{6}$$

$$E_2 = \sqrt{\frac{1}{n-1}\sum_{i=1}^{n}(r_i - E_1)^2} \tag{7}$$

where $r_i = f_{pred} - f_{exp}/f_{exp}$ and n is the number of the experimental data. E_1 is the average absolute percent error, which is used to estimate the agreement between predicted and measured data. E_2 is the standard deviation of the average absolute percent error, which is used to evaluate the prediction capability of models and correlations.

The statistical parameters (E_1 and E_2) of different models are presented in Table 3. It can be found that the Metkin and Sokolov's correlation gives the best performance with an average absolute percent error of 16.39% and the standard deviation of the average absolute percent error of 6.04%. Descamps et al.'s correlation shows the worst performance with 72.04 and 12.63%. Although Metkin and Sokolov's correlation gives a relatively small error compared with other models, E_1 is still up to 16.39%. Considering the operating conditions in this work (u_{sg} ranged from 0.04 to 0.34 m/s and u_{sl} ranged from 0 to 2 m/s), to calculate exactly the fraction factor, a model based on the work of Herringe and Davis (1978) with the correlation of liquid friction factor (f_m/f_l) is suggested as

Table 3. Statistical Parameters of the Different Correlations for Gas–Liquid Friction Factor

correlation	E_1 (%)	E_2 (%)
Herringe & Davis	36.04	43.47
Metkin & Sokolov	16.39	6.04
Descamps et al.	72.04	12.63
Xu et al.	54.58	24.40
this work	9.92	5.75

$$\frac{f_m}{f_l} = 0.68 + 3.78\alpha_g - 3.35\alpha_g^2 \tag{8}$$

As Table 3 shows, the model gives a reasonable performance with E_1 9.92% and E_2 5.75%. Figure 10 shows a comparison of the predicted friction factor with the experimental data. It is clear that the predicted friction factors by using the Poiseuille relations underestimate the experimental values as the mixture Reynolds number decreases. By contrast, the new correlation proposed in this work provides reasonable predictions for the relevant experimental data. Therefore, this new model applies to gas–liquid two-phase flow.

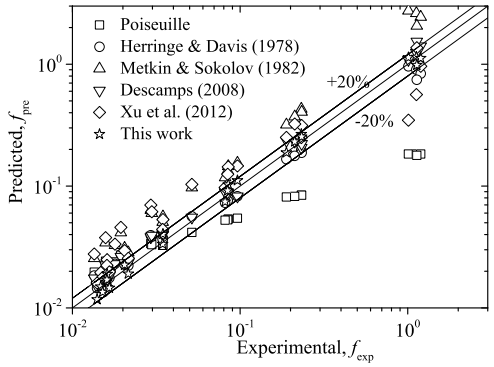

Figure 10. Comparison of the measured and predicted friction factors for the oil–gas two-phase flow.

In terms of sensitivity of the correlation proposed here, according to error propagation proposed by Bevington and Roinson,[25] the error propagation of predicted f_m can be expressed as

$$\Delta f_m = \left[3.78\frac{u_{sl}\Delta u_{sg} - u_{sg}\Delta u_{sl}}{(u_{sl}+u_{sg})^2} - 6.7u_{sg}\frac{u_{sl}\Delta u_{sg} - u_{sg}\Delta u_{sl}}{(u_{sl}+u_{sg})^3}\right] f_l + \left[0.68 + 3.78\frac{u_{sg}}{u_{sl}+u_{sg}} - 3.35\left(\frac{u_{sg}}{u_{sl}+u_{sg}}\right)^2\right]\Delta f_l \tag{9}$$

in which, Δ refers to the error range of certain parameter. According to eq 9, under experimental conditions, the uncertainty bought by rotameter, electro-magnetic flowmeter, and pressure sensor results in an uncertainty range of f_m between 0.0005 and 0.0013. In particular, 1% variance of u_{sg} results in less than 1.06% variance of f_m value, and 1% variance of u_{sl} value results in less than 1.14% variance of f_m value.

Figure 11 presents the experimental friction factor for oil containing sand and gas flow as a function of the mixture Reynolds number. Compared with the oil–gas two-phase flow, the three-phase flow friction factors are lower for pure oil when the gas superficial velocity is lower than 0.17 m/s at a given volume concentration of 2%. This implies that the presence of gas increases the friction factor. However, when some sand was added in the oil–gas two-phase flow, the friction factor decreased.

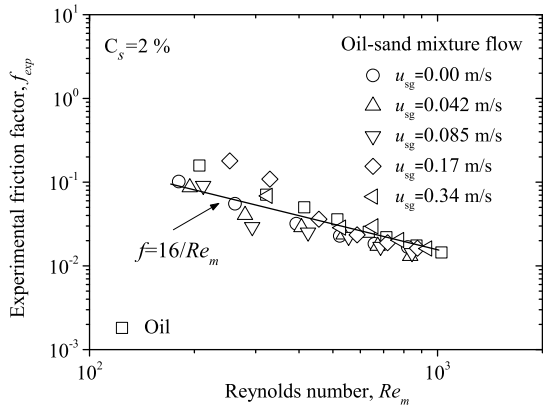

Figure 11. Experimental friction factor versus Reynolds number in the laminar flow for oil–sand–gas three-phase flow.

https://dx.doi.org/10.1021/acsomega.0c04637
ACS Omega XXXX, XXX, XXX–XXX

Figure 12 shows a comparison of the predicted friction factor by using eq 8 with the experimental friction factor of the oil containing sand and gas flow at a constant volume concentration of 2%. Compared with the friction factor predicted by the Poiseuille relations and other correlations, the method gives reasonable predictions for the relevant experimental data when the fraction factor is larger and the error falling with the ±20% range. The important cause that formed the relatively large error (±20%) lies in the sand particle's volume concentration, which will be lower when the velocity is small. Considering that a more accurate prediction of the pressure gradient in the three-phase flow is greatly complicated and difficult, the method suggested in this work is good to be applied in oil containing sand and gas pipe flow.

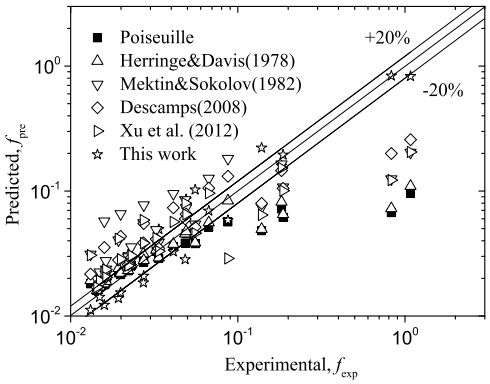

Figure 12. Comparison of the measured and predicted friction factors for oil−sand−gas three-phase flow.

CONCLUSIONS

The pressure gradient characteristics in the hydraulic oil containing sand and air flow along vertical pipelines was studied in consideration of non-Newtonian properties. Moreover, the effect of sand size distribution and volume concentration on the rheological properties and the vertical pipe flow pressure gradient was also investigated.

The rheology measurements demonstrated that hydraulic oil containing sand exhibits shear-thinning behavior. When hydraulic oil was blended with a small amount of sand, the

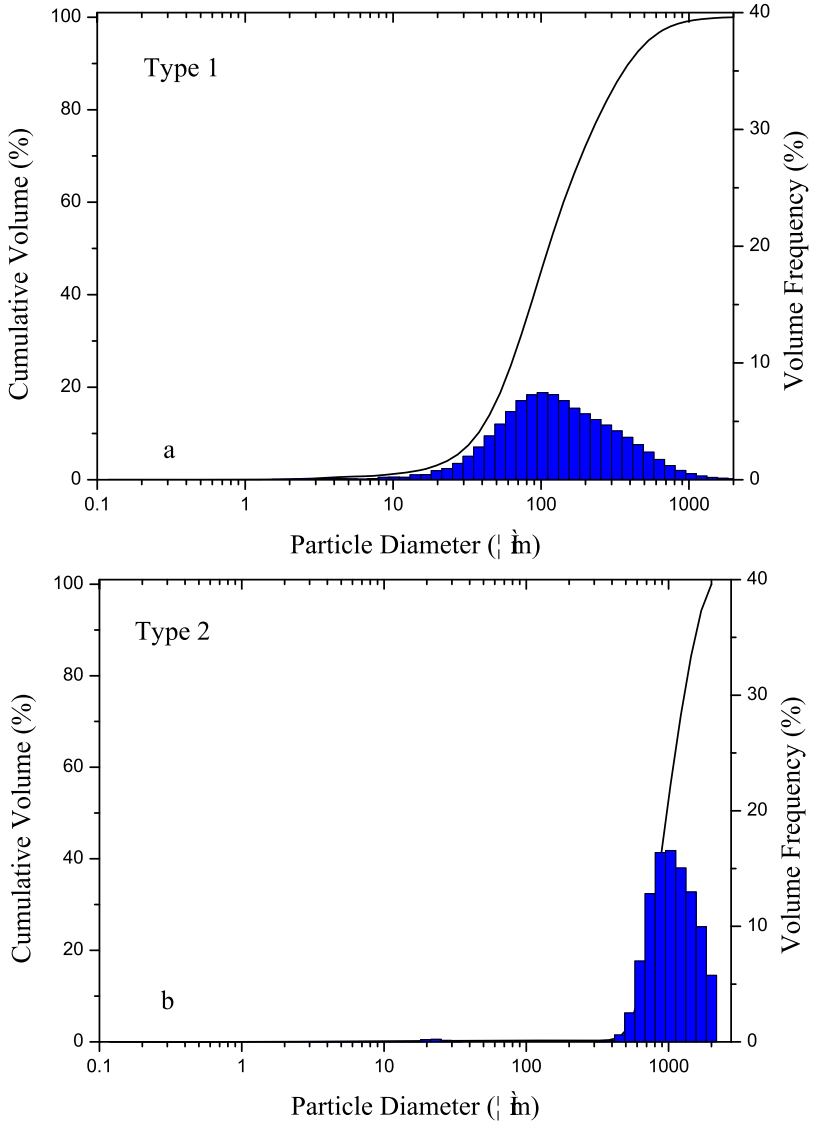

Figure A1. Sand size distributions of the two types.

https://dx.doi.org/10.1021/acsomega.0c04637
ACS Omega XXXX, XXX, XXX−XXX

apparent viscosity of the mixture decreased, so that a low pressure drop appeared in the pipe flow. By comparing the rheological measurements and laminar pipe flow data, the flow curves measured by the rheometer could be used to predict the shear stress in the pipe flow.

It was demonstrated that gas injection can markedly decrease the total pressure drop of hydraulic oil containing sand at a low mixture velocity. However, when the superficial oil velocity increased, the effect of gas injection on drag reduction will diminish. Furthermore, for the total pressure gradient, the presence of gas decreased the gravity pressure gradient considerably, and thus the total pressure gradient decreased. Regarding hydraulic flow, gas injection can change the friction factor; moreover, the frictional pressure drop initially decreased and then gradually increased as the superficial oil velocity increased. Compared to the friction factor predicted by the Poiseuille relations, the model proposed in this work provided reasonable predictions for the relevant experimental data.

EXPERIMENTAL SECTION

Materials. Hydraulic oil was used to study the flow characteristics in vertical tubes. At a temperature of 23 °C, the oil was found to have a density of 828 kg/m^3. The sand size and its distribution were measured by a Malvern Insitec SX Laser particle size analyzer. To study the effect of sand size distribution on the flow properties, two different types of distributions were used. Figure A1 shows the sand size distributions of these two types; several basic properties are summarized in Table A1. In Table A1, D5, D95, and D50 describe the sand particle size distribution together. D_5 means diameter larger than 5% of all sand particles recorded. D_{50} means diameter larger than 50% of all sand particles recorded. It is the median particle size as well. D_{95} means diameter larger than 95% of all sand particles recorded. The oil blended with sand was classified as sample 1 if it contained type 1 sand and sample 2 if it contained type 2 sand. Type 1 was used to study the effect of sand volume concentration on the rheology and flow characteristics. The hydraulic oil was blended with sand in three different volume concentrations, namely, 0.7, 2, and 3%.

Table A1. Several Basic Properties of Sands for Two Different Types

no.	density of sediment grains ρ_s (kg/m^3)	D_5 (μm)	D_{50} (μm)	D_{95} (μm)
type 1	2391	26	112.24	534
type 2	2480	569.65	1073.65	1809.62

Rheological Measurements. Prior to the pipe flow experiments, rheological measurements were carried out using a Haake RS6000 rheometer. A coaxial cylinder sensor system (Z38 DIN, gap width of 2.5 mm, and sample volume of 30.8 cm^3) was used to determine the rheological properties. In this equipment, the liquid temperature-controlled system lets the sensor reach a fixed temperature and maintains it through the experiment. In the measurements, the samples were prepared in batches of 300 mL and preheated to a fixed test temperature, and then homogenization of oil and sand was achieved by using a three-blade stirrer at a fixed low speed. After homogenization, the rheological properties of the samples were determined by using the rheometer. In the viscosity measurement, the viscosity curves were obtained by increasing the shear rate from 0 to 100 s^{-1} over a period of 100 s at a fixed temperature.

Pipe Flow Experiments. The equipment is schematically shown in Figure A2. The flow rate, pressure drop, and flow patterns can be obtained by this test loop. The test flow pipeline was constructed using a perspex tube with an inner diameter of 50 mm, a total length of 14 m, and a vertical length of 3 m. Air came from a compressor pump via a filter, a control valve, and a rotameter with 2.5% grade of accuracy. The loop consisted of a 300 L main mixing tank, where the solid and the liquid were mixed homogeneously and introduced into the test

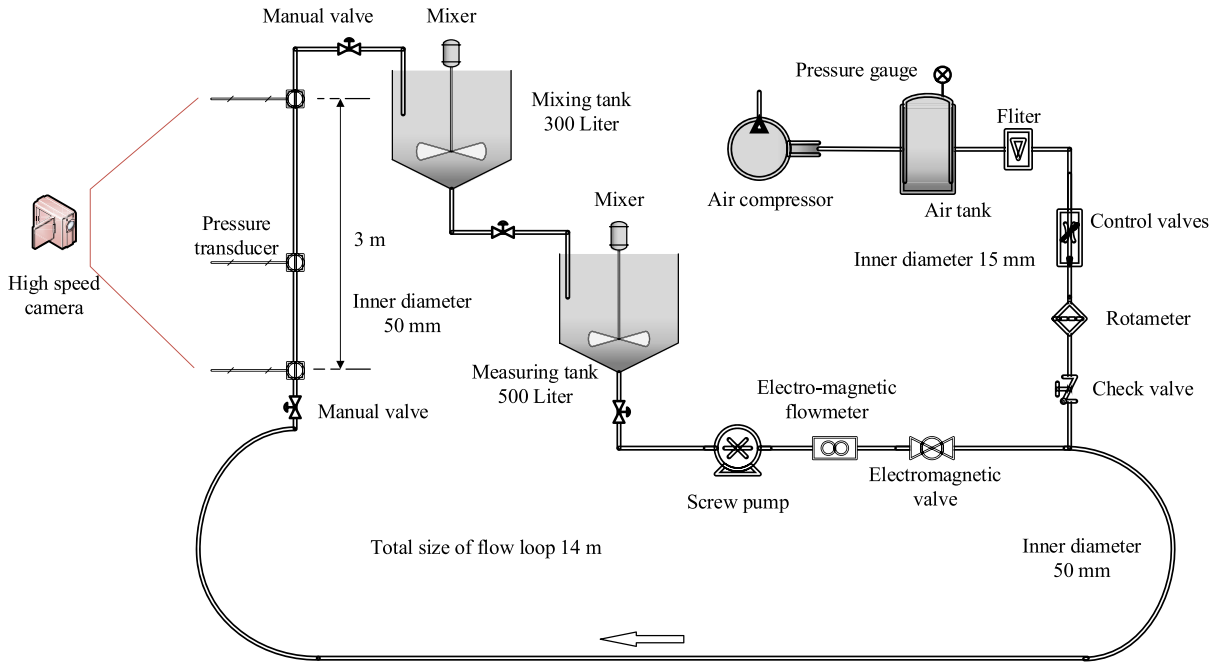

Figure A2. Schematic view of the flow loop.

https://dx.doi.org/10.1021/acsomega.0c04637
ACS Omega XXXX, XXX, XXX−XXX

loop. A 500 L measuring tank was employed to determine the delivered volumetric solid fraction and the oil or oil−sand mixture flow rate. A centrifugal pump was used to transfer the slurry at velocities between 0 and 3 m/s. To achieve various velocities, a frequency inverter was used to control the centrifugal pump, and an electro-magnetic flowmeter with 1% grade of accuracy was applied to measure the flow rate of liquid phases. The pressure drop in the test section was measured by Honeywell 40CP100G absolute pressure transducers, whose grade of accuracy was 0.4% under experiment operating conditions. Moreover, the oil−sand mixture is sampled at the entrance and exit of the testing section to test the sand concentration. In most cases, the relative deviation of the sand concentration between the entrance and exit is less than 5%, meaning the mixture is relatively stable.

APPENDIX

Methods of Data Analysis

Rheological Property. As expected, the oil and oil−sand mixture in this study are shear-thinning fluids whose rheological properties can be described by fitting the experimental data to the power-law model. This model can be described using two parameters as follows

$$\tau = k(\dot{\gamma})^n \tag{A.1}$$

where τ and $\dot{\gamma}$ denote the shear stress in Pa and the shear rate in s^{-1}, respectively. k and n are two empirical curve-fitting parameters called the fluid consistency coefficient (in Pa·s^n) and the flow behavior index, respectively. According to eq A.1, the appropriate model parameters can be determined by using the least-squares method. The two parameters extrapolated by the power-law model are listed in Table A1, where it can be seen that the power-law model yields a high regression correlation coefficient ($R^2 \geq 0.998$).

Pipe Vertical Flow. For a fully developed mixture flow in a vertical pipe (neglecting the acceleration gradient), the total pressure gradient includes the gravity pressure gradient and the frictional pressure gradient, namely

$$\left(\frac{dp}{dl}\right)_{total} = \left(\frac{dp}{dl}\right)_g + \left(\frac{dp}{dl}\right)_f \tag{A.2}$$

$$\left(\frac{dp}{dl}\right)_g = \rho_m g \tag{A.3}$$

$$\left(\frac{dp}{dl}\right)_f = F_l + F_{gl} \tag{A.4}$$

where ρ_m, g, and α_g are the mixture density, the gravitational acceleration, and the input gas fraction, respectively. In eq A.4, F_l is the frictional pressure gradient for the mixture liquids flowing alone in the vertical pipe. F_{gl} is the gas−liquid (oil or oil−sand mixture) frictional pressure that accounts for bubble agitation.

Assuming nonslip between the sand and the liquid phase, the homogeneous flow model can be applied to sand−oil flow. Homogeneous mixture properties such as density can be calculated by the following equation

$$\rho_l = (1 - C_s)\rho_o + C_s\rho_s \tag{A.5}$$

where ρ_o and ρ_s are the density of oil and sand, respectively. C_s is the volume concentration of the sand.

García et al.[26] presented an experiment to study the relationship between the mixture Fanning friction factor and the mixture Reynolds number. The Fanning friction factor for the two-phase or three-phase mixture flow is defined as

$$f_m = \frac{(dp/dl)_f D}{2\rho_m u_m^2} \tag{A.6}$$

$$u_m = u_{sg} + u_{sl} \tag{A.7}$$

$$\rho_m = \alpha_g\rho_g + (1 - \alpha_g)\rho_l \tag{A.8}$$

where u_m is the mixture velocity, that is, the sum of the superficial gas and mixture liquid velocities. ρ_m is the mixture density. In a fully developed and steady flow of an incompressible fluid in a pipe, the frictional factor can be expressed in terms of the Reynolds number as:

$$f_m = \frac{16}{Re_m}, \text{ in a laminar flow} \tag{A.9}$$

$$f_m = \frac{0.079}{Re_m^{0.25} Re_m^{0.25}}, \text{ in a turbulent flow} \tag{A.10}$$

where the mixture Reynolds number Re_m is defined as

$$Re_m = \frac{\rho_m u_m D}{\mu_m} \tag{A.11}$$

where $\mu_m = \alpha_g\mu_g + (1 - \alpha_g)\mu_{al}$ is a composite viscosity related to the flow rate fraction.

According to Zhang and Xu,[27] for a power-law fluid[28] (oil or oil−sand mixture), the mixture viscosity μ_{al} (also called apparent viscosity) is defined as

$$\mu_{al} = D^{1-n} 8^{n-1} u_{sl}^{n-1} k\left(\frac{1 + 3n}{4n}\right)^n \tag{A.12}$$

The wall shear stress can be related to the frictional pressure drop through the following equations

$$\tau_w = \frac{(dp/dl)_f D}{4} \tag{A.13}$$

The wall shear rate in a laminar power-law fluid flow can be obtained as follows[29]

$$\dot{\gamma}_w = \frac{32Q_m}{\pi D^3}\left(\frac{1 + 3n}{4n}\right) \tag{A.14}$$

where Q_m denotes the mixture flow rate. Thus, in a laminar flow, the shear stress and the shear rate can be obtained by measuring the frictional pressure drop and the flow rate.

AUTHOR INFORMATION

Corresponding Authors

Shuo Liu − *Institute of Mechanics, Chinese Academy of Sciences, Beijing 100190, China*; Phone: 008620-82544173; Email: liushuo@imech.ac.cn

Jing-yu Xu − *Institute of Mechanics, Chinese Academy of Sciences, Beijing 100190, China; School of Engineering Sciences, University of Chinese Academy of Sciences, Beijing 100049, China*; orcid.org/0000-0002-1058-2257; Phone: 008610-82544179; Email: xujingyu@imech.ac.cn

https://dx.doi.org/10.1021/acsomega.0c04637
ACS Omega XXXX, XXX, XXX−XXX

Authors

Dong Zhang − *Institute of Mechanics, Chinese Academy of Sciences, Beijing 100190, China; Sinopec Research Institute of Petroleum Engineering, Beijing 100101, China*

Jian Zhang − *Institute of Mechanics, Chinese Academy of Sciences, Beijing 100190, China*

Lin-tong Hou − *Institute of Mechanics, Chinese Academy of Sciences, Beijing 100190, China; School of Engineering Sciences, University of Chinese Academy of Sciences, Beijing 100049, China*

Complete contact information is available at: https://pubs.acs.org/10.1021/acsomega.0c04637

Notes

The authors declare no competing financial interest.

■ ACKNOWLEDGMENTS

The authors gratefully acknowledge that the work described here is financially supported by the National Natural Science Foundation of China (no. 51779243) and the Strategic Priority Research Program of the Chinese Academy of Science (grant no: XDB22030101).

■ REFERENCES

(1) Almedeij, J. H.; Algharaib, M. K. Influence of sand production on pressure drawdown in horizontal wells: Theoretical evidence. *J. Petrol. Sci. Eng.* **2005**, *47*, 137−145.

(2) Adeyanju, O. A.; Oyekunle, L. O. Hydrodynamics of sand-oil-gas multiphase flow in a near vertical well. *SPE Annual Technical Conference and Exhibition*, Lagos.

(3) Stevenson, P.; Thorpe, R. B.; Kennedy, J. E.; McDermott, C. The transport of particles at low loading in near horizontal pipes by intermittent flow. *Chem. Eng. Sci.* **2001**, *56*, 2149−2159.

(4) Dusseault, M. B.; EI-Sayed, S. Heavy oil production enhance by encouraging sand production. *SPE/DOE, Improved Oil Recovery Symposium*, Tulsa.

(5) Radin, I.; Zakin, J. L.; Patterson, G. K. Drag reduction in solid-fluid systems. *AIChE J.* **1975**, *21*, 358−371.

(6) Wang, Y.; Yu, B.; Zakin, J. L.; Shi, H. Review on drag reduction and its heat transfer by additives. *Adv. Mech. Eng.* **2011**, *3*, 478749.

(7) Zhang, J.; Chen, X.-p.; Zhang, D.; Xu, J.-y. Rheological behavior and viscosity reduction of heavy crude oil and its blends from the Suizhong oilfield in China. *J. Petrol. Sci. Eng.* **2017**, *156*, 563−574.

(8) Javdani, K.; Schwalbe, S.; Fischer, J. Liquid or slurry holdup in the flow of gas-liquid and gas-slurry mixtures in vertical tubes. *Fuel Process. Technol.* **1978**, *1*, 287−296.

(9) Kim, S. D.; Choi, J. H. Three phase flow of gasndashcoal slurry mixtures in vertical tubes. *Can. J. Chem. Eng.* **1984**, *62*, 85−90.

(10) Miller, R. L.; Cain, M. B. Prediction of flow regime transitions in vertical upward three phase gas-liquid-solid flow. *Chem. Eng. Commun.* **1986**, *43*, 147−163.

(11) Erian, F. F.; Pease, L. F. Three-phase upward flow in a vertical pipe. *Int. J. Multiphas. Flow* **2007**, *33*, 498−509.

(12) Xu, J.-y.; Zhang, J.; Liu, H.-f.; Wu, Y.-x. Oil-gas-water three-phase upward flow through a vertical pipe: Influence of gas injection on the pressure gradient. *Int. J. Multiphas. Flow* **2012**, *46*, 1−8.

(13) Rahman, M. A.; Adane, K. F.; Sanders, R. S. An improved method for applying the Lockhart-Martinelli correlation to three-phase gas-liquid-solid horizontal pipeline flows. *Can. J. Chem. Eng.* **2013**, *91*, 1372−1382.

(14) Dziubinski, M.; Fidos, H.; Sosno, M. The flow pattern map of a two-phase non-Newtonian liquid-gas flow in the vertical pipe. *Int. J. Multiphas. Flow* **2004**, *30*, 551−563.

(15) Zhang, J.; Wu, Q.-l.; Liu, S.; Xu, J.-y. Investigation of the Gas−Liquid Two-Phase Flow and Separation Behaviors at Inclined T-Junction Pipelines. *ACS Omega* **2020**, *5*, 21443−21450.

(16) Gillies, R. G.; McKibben, M. J.; Shook, C. A. Pipeline flow of gas, liquid and sand mixtures at low velocities. *J. Can. Petrol. Technol.* **1997**, *36*, 36−42.

(17) Al-Sarkhi, A.; Hanratty, T. J. Effect of Pipe Diameter on the Performance of Drag-Reducing Polymers in Annular Gas-Liquid Flows. *Chem. Eng. Res. Des.* **2001**, *79*, 402−408.

(18) Al-Sarkhi, A.; Abu-Nada, E.; Batayneh, M. Effect of drag reducing polymer on air−water annular flow in an inclined pipe. *Int. J. Multiphas. Flow* **2006**, *32*, 926−934.

(19) Al-Sarkhi, A.; Hanratty, T. J. Effect of drag-reducing polymers on annular gas−liquid flow in a horizontal pipe. *Int. J. Multiphas. Flow* **2001**, *27*, 1151−1162.

(20) Fernandes, R. L. J.; Jutte, B. M.; Rodriguez, M. G. Drag reduction in horizontal annular two-phase flow. *Int. J. Multiphas. Flow* **2004**, *30*, 1051−1069.

(21) Herringe, R. A.; Davis, M. R. Flow structure and distribution effects in gas-liquid mixture flows. *Int. J. Multiphas. Flow* **1978**, *4*, 461−486.

(22) Marié, J. L. Modeling of the skin friction and heat transfer in turbulent two-component bubbly flows in pipes. *Int. J. Multiphas. Flow* **1987**, *13*, 309−325.

(23) Descamps, M. N.; Oliemans, R. V. A.; Ooms, G.; Mudde, R. F. Air-water flow in a vertical pipe: experimental study of air bubbles in the vicinity of the wall. *Exp. Fluid* **2008**, *45*, 357−370.

(24) Metkin, V. P.; Sokolov, V. N. Hydraulic resistance to flow of gas-liquid mixtures having non-Newtonian properties. *Russ. J. Appl. Chem.* **1982**, *55*, 558−563.

(25) Bevington, P. R.; Robinson, O. K. *Data Reduction and Error Analysis for the Physical Sciences*, 3rd ed.; McGraw-Hill Press: Boston, 2003; pp 39−40.

(26) García, F.; García, R.; Padrino, J. C.; Mata, C.; Trallero, J. L.; Joseph, D. D. Power law and composite power law friction factor correlations for laminar and turbulent gas-liquid flow in horizontal pipelines. *Int. J. Multiphas. Flow* **2003**, *29*, 1605−1624.

(27) Zhang, J.; Xu, J. Y. Rheological behavior of oil and water emulsions and their flow characteristics in horizontal pipes. *Can. J. Chem. Eng.* **2016**, *94*, 324−331.

(28) Hou, L.-t.; Liu, S.; Zhang, J.; Xu, J.-y. Evaluation of the Behavioral Characteristics in a Gas and Heavy Oil Stratified Flow According to the Herschel-Bulkley Fluid Model. *ACS Omega* **2020**, *5*, 17787−17800.

(29) Zhang, D.; Liu, S.; Zhang, J.; Xu, J. Y. Rheological properties of heavy crude oil containing sand from Bo-hai oilfield in China. *Appl. Rheol.* **2017**, *27*, 10−18.

https://dx.doi.org/10.1021/acsomega.0c04637
ACS Omega XXXX, XXX, XXX−XXX